MOTIFNet: Automating the Analysis of Amphiphile and Block Polymer Self-Assembly from SAXS Data

Daoyuan Li
University of Minnesota
li002504@umn.edu

Shuquan Cui
University of Minnesota
cui00123@umn.edu

Mahesh K. Mahanthappa
University of Minnesota
maheshkm@umn.edu

Frank S. Bates
University of Minnesota
bates001@umn.edu

Timothy P. Lodge
University of Minnesota
lodge@umn.edu

J. Ilja Siepmann
University of Minnesota
siepmann@umn.edu

Abstract

Accurately classifying morphology and assessing stability in soft matter self-assembly often require specialized analysis of small-angle X-ray scattering (SAXS) data, creating an obstacle to automation. To address this, we introduce MOTIFNet, a simplified sparse mixture of experts (MoE) model with top-1 routing. By combining temporal convolution and self-attention, MOTIFNet effectively processes SAXS time series data, enabling morphology classification, SAXS pattern prediction, and the estimation of order-disorder transition (ODT) probabilities. This model advances automated characterization, accelerating experimentation and high-throughput studies in soft matter self-assembly.

1 Introduction

Amphiphilic molecules and block polymers can self-assemble into a diverse range of morphologies, including but not limited to body-centered cubic (BCC), double diamond (DD), double gyroid (DG), hexagonally packed cylindrical (HEX), lamellar (LAM), O70, and Q214. These self-assembled structures play crucial roles in determining the material properties and have been explored extensively in both computational and experimental studies [1–4]. Rapidly identifying these morphologies and ensuring that the assembled system remains stable over specific future time periods are pivotal steps in translating these materials into industrial applications [5, 6].

Among the various experimental techniques used to analyze self-assembled morphologies, small-angle X-ray scattering (SAXS) stands out as a crucial method for both identifying morphology types and detecting order-disorder transitions (ODTs) [7]. Its numerical analogs have become essential tools in computational exploration [8, 9]. However, SAXS analysis traditionally relies on specialized knowledge and manual peak annotation, a process that is not only time-consuming but also demands considerable experience. The challenge intensifies when it comes to predicting SAXS time series data, which significantly hinders the automated characterization and high-throughput exploration of soft matter self-assembly. This bottleneck limits the scalability of SAXS-based studies and poses a substantial barrier to advancing the field.

To address these challenges, we designed the attention-enhanced temporal convolution network (ATCN), which builds upon the temporal convolutional network (TCN) architecture [10]. Our approach integrates a multi-head self-attention layer between two adjacent temporal convolution layers to enhance the model's ability to capture relationships among different features [11, 12]. This design enables the model to better learn the characteristic ratios of SAXS peaks.

38th Conference on Neural Information Processing Systems (NeurIPS 2024).

Building on ATCN, we developed the morphological order-disorder transition identification and forecasting network (MOTIFNet), a simplified mixture of experts (MoE) model [13, 14]. In MOTIFNet, we employ a top-1 router to dynamically select from 7 experts, each specialized in one morphology, thus enabling more accurate and efficient SAXS analysis in soft matter self-assembly.

2 Related Work

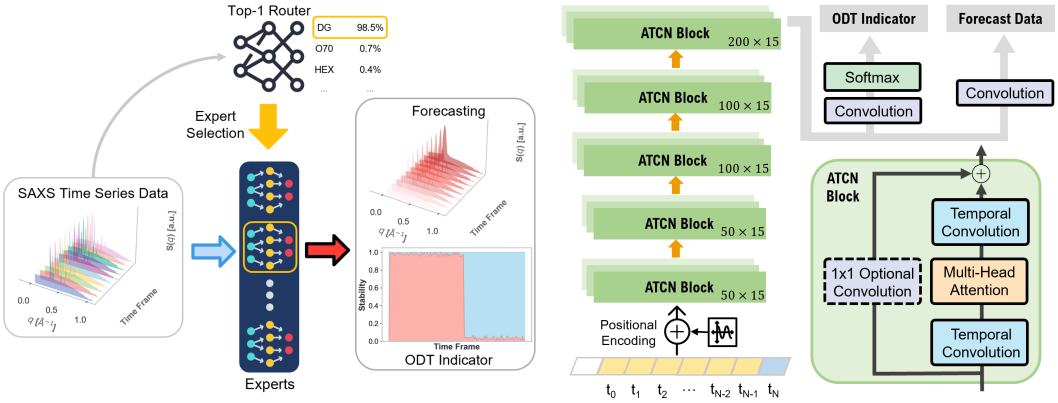

Figure 1: MOTIFNet (left) and the detailed architecture of the expert module (right).

The application of deep learning to accelerate research in soft matter self-assembly has gained significant traction in recent years. For instance, deep learning models like PointNet have been employed to detect ordered morphologies from molecular simulations [15, 16]. Additionally, CNNs designed with feature engineering based on discrete Fourier transforms have leveraged the periodicity inherent in self-assembled structures [17]. Other notable approaches have further expanded this domain [18–20]. Additionally, machine learning has been employed in SAXS data analysis for tasks such as protein reconstruction and morphology identification [21–23].

TCNs have obtained prominence in time series analysis due to their excellent parallelization capabilities and relatively low training costs [10]. However, due to their reliance on one-dimensional convolutions, TCNs often struggle to effectively capture relationships across different features. To mitigate this limitation, recent studies have explored enhancing TCNs' ability to recognize feature dependence by integrating attention mechanisms [24, 25].

The MoE paradigm has been proven effective across a variety of fields, especially in natural language processing tasks [26]. In particular, the use of sparse activation models, such as those employing a top-1 router, has demonstrated considerable success in improving efficiency and scalability [27].

3 Methods

Synthetic data preparation To train and evaluate our model, we generated synthetic SAXS time series data corresponding to 7 morphologies: BCC, DD, DG, HEX, LAM, O70, and Q214. For each morphology, we calculated the characteristic peak ratios based on their respective space groups [28], and determined the position ranges, heights, and widths of the primary peak according to empirical experimental knowledge. Peaks were modeled using Gaussian wave packets. To improve the generalization and robustness of the model, random noise was introduced into the data. The ODTs were designed based on experimental observations, characterized by a decrease in the primary peak height, an increase in its width, and the gradual disappearance of other peaks. During an ODT, the primary peak experienced a ±3% shift, with the magnitude of this shift following a bimodal normal distribution. To ensure reliable model evaluation, the generated data was split into training and testing sets, with 80% of the data allocated for training and the remaining 20% used for testing.

Model design MOTIFNet is composed of 7 experts and a top-1 router, all based on the ATCN architecture, as illustrated in Figure 1. Each expert in the network is specialized in processing SAXS data corresponding to one morphology. The top-1 router is responsible for dynamically selecting

the most appropriate expert for a given input, effectively acting as a morphology classifier. This approach reduces training and operational costs, enhances the modularity of the model—facilitating the potential inclusion of additional morphologies—and improves interpretability.

The router is constructed using 3 ATCN blocks with channel sizes of 32, 64, and 128, and a kernel size of 5. Following the ATCN blocks, convolutional layers are applied to further process the features, and a softmax layer to produce a 7-class output. The architecture of the expert is shown in Figure 1.

Logarithmic and exponential transformations To handle the variability in the magnitude of the input data, a logarithmic transformation is applied to each element X_{ijt} in the input sequence:

$$\tilde{X}_{ijt} = \log(1 + \max(X_{ijt}, 0))$$

This transformation ensures that all inputs are non-negative, facilitating stable logarithmic operations. After the network produces the output $\hat{Y}'$, the inverse transformation is applied to restore the data to its original scale as $\hat{Y}_{ijt} = \exp(\min(\hat{Y}'_{ijt}, 10)) - 1$. The minimum operation prevents excessively large values that could destabilize training or inference.

Attention-enhanced temporal convolution network (ATCN) Each ATCN block outputs a transformed tensor with the same dimensions as the input. The temporal convolution is defined as:

$$\text{Conv1D}_{k,d}^{\text{Causal}}(X)_{ijt} = \sum_{s=0}^{k-1} W_{js} \cdot X_{i,j,t-ds} \cdot \mathbb{I}(t - ds \geq 0)$$

where k is the kernel size, d is the dilation rate, and W_{js} represents the convolutional filter weights. The indicator function $\mathbb{I}(t - ds \geq 0)$ ensures the convolution only considers current and past time steps, preserving temporal causality.

The multi-head attention mechanism applied to queries Q, keys K, and values V is denoted as $\text{Attn}(Q, K, V)$. The operations within an ATCN block can be summarized as:

$$Y_{\text{output}} = \sigma\left(\text{Conv1D}_{k_2,d_2}^{\text{Causal}}\left(\text{Attn}\left(Y_1, Y_1, Y_1\right)\right) + \mathbb{I}(N \neq N') \cdot \text{Conv1D}_{1,1}(X) + \mathbb{I}(N = N') \cdot X\right)$$

where $Y_1 = \text{Conv1D}_{k_1,d_1}^{\text{Causal}}(X)$ is the output of the first convolution, implicitly adjusted to match the input length by removing excess padding, σ is a non-linear activation function (typically ReLU), and $\mathbb{I}(N \neq N')$ applies a 1×1 convolution if the input and output dimensions differ, ensuring compatibility in residual connections [29].

Loss function The expert is trained using two loss functions: RMSE for SAXS data prediction and cross-entropy loss for binary ODT classification. The total loss is: $\mathcal{L} = \mathcal{L}_{\text{SAXS}} + \lambda \mathcal{L}_{\text{ODT}}$, where λ is a hyperparameter balancing the importance of the SAXS prediction and the ODT classification.

Table 1: Performance comparison

	Models		
Performance	CNN	TCN	**ATCN**
Classification (accuracy)	0.98	0.97	**0.99**
ODT indication (accuracy)	0.69	0.77	**0.83**
SAXS prediction (RMSE loss)	175.6	85.3	**19.1**

4 Results and Discussion

In our experiments, we compared the performance of 3 neural network architectures—CNN, TCN, and ATCN—in constructing MOTIFNet and evaluated their effectiveness on the synthetic dataset. The layers, channel sizes, and kernel sizes for all 3 models were kept consistent with those depicted in Figure 1. As shown in Table 1, the ATCN-based MOTIFNet outperforms the other 2 architectures across all tasks, particularly excelling in ODT indicator accuracy and SAXS prediction.

MOTIFNet demonstrated high performance, as illustrated in Figure 2, where the top-1 router achieved nearly 100% classification accuracy, which ensures that the input data is reliably assigned to the corresponding expert. The ODT indicator also showed high accuracy, calculated on a per-time-step basis. However, its performance was slightly weaker during the time steps where an ODT is about to

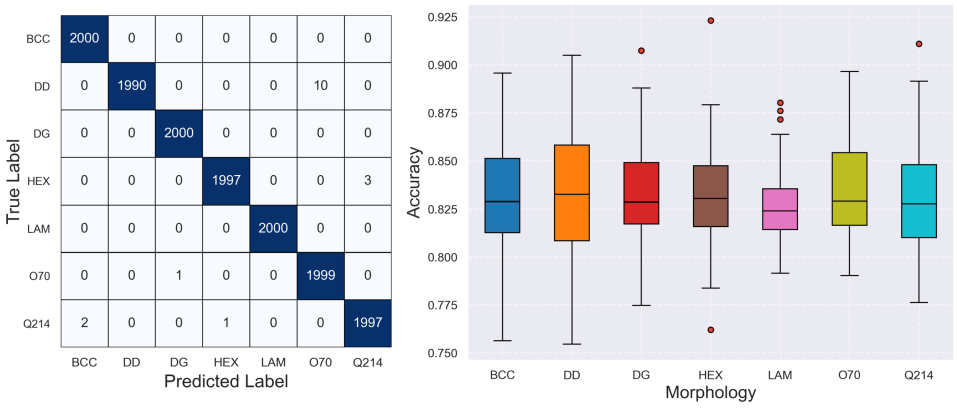

Figure 2: (left) Confusion matrix of the router. (right) Accuracy of ODT indicators.

begin or end, which lowers the overall accuracy. The DD morphology exhibited greater variance in accuracy due to more dramatic peak height decreases during the ODT, as the peaks in DD are much taller than other morphologies.

To further explore the interpretability of MOTIFNet, we employed integrated gradients on numerical SAXS data from molecular simulations of the DG morphology, as shown in Figure 3 [30]. We computed the feature importance, corresponding to the horizontal axis q in SAXS. The DG structure, associated with the Ia$\bar{3}$d space group symmetry, is characterized by peak ratios at $\sqrt{6}, \sqrt{8}, \sqrt{16}, \sqrt{20}, \sqrt{22}, \sqrt{24}, \sqrt{26}, \sqrt{48}$ [28]. For this molecular system, the peaks at $\sqrt{6}, \sqrt{8}, \sqrt{20}, \sqrt{22}, \sqrt{24}, \sqrt{26}$ are particularly prominent.

In comparison to TCN, the feature importance heatmap obtained from ATCN's integrated gradients analysis reveals that ATCN effectively captures these significant peaks, aligning closely with the expected peak positions in the simulated DG data. Specifically, ATCN correctly identifies the key peaks in the DG morphology, which the TCN fails to highlight with the same accuracy. This observation underscores ATCN's enhanced interpretability and reliability in identifying morphological features inherent to the DG structure, thereby validating the interpretability of MOTIFNet.

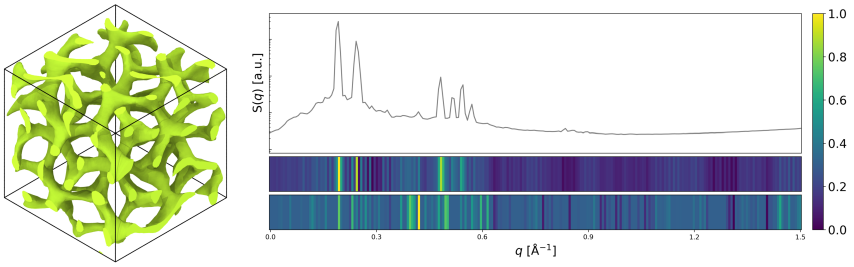

Figure 3: (left) Simulation snapshot of DG morphology. (right) Numerical SAXS from molecular simulation and integrated gradients analysis. Upper heatmap: ATCN; Lower heatmap: TCN.

5 Conclusions

In this work, we designed the ATCN and utilized it as the foundation for MOTIFNet, a model tailored for the classification, stability assessment, and pattern prediction of SAXS time series data. By simplifying the MoE architecture, MOTIFNet provides modularity, lightweight implementation, and exceptional performance on synthetic datasets. It also demonstrated strong performance in simulation data. We believe that MOTIFNet has the potential to significantly accelerate the automated characterization of soft matter self-assembly, offering valuable insights for the analysis of other time series data from spectroscopic measurements. The model's adaptability and strong performance suggest that it could become a vital tool in both computational and experimental studies, paving the way for further advancements in high-throughput materials research.

References

[1] Qile P Chen, Leonel Barreda, Luis E Oquendo, Marc A Hillmyer, Timothy P Lodge, and J Ilja Siepmann. Computational design of high-χ block oligomers for accessing 1 nm domains. *ACS nano*, 12(5):4351–4361, 2018.

[2] Zhengyuan Shen, Jingyi L Chen, Viktoriia Vernadskaia, S Piril Ertem, Mahesh K Mahanthappa, Marc A Hillmyer, Theresa M Reineke, Timothy P Lodge, and J Ilja Siepmann. From order to disorder: computational design of triblock amphiphiles with 1 nm domains. *Journal of the American Chemical Society*, 142(20):9352–9362, 2020.

[3] Shuquan Cui, Bo Zhang, Liyang Shen, Frank S Bates, and Timothy P Lodge. Core–shell gyroid in abc bottlebrush block terpolymers. *Journal of the American Chemical Society*, 144(47):21719–21727, 2022.

[4] Shuquan Cui, Elizabeth Murphy, Wei Zhang, Aristotelis Zografos, Liyang Shen, Frank Bates, and Timothy Lodge. Rectangular centered cylinders-in-undulating-lamellae from abc bottlebrush block terpolymers. *Bulletin of the American Physical Society*, 2024.

[5] Frank S Bates, Marc A Hillmyer, Timothy P Lodge, Christopher M Bates, Kris T Delaney, and Glenn H Fredrickson. Multiblock polymers: Panacea or pandora's box? *Science*, 336(6080):434–440, 2012.

[6] Deborah K Schneiderman and Marc A Hillmyer. 50th anniversary perspective: there is a great future in sustainable polymers. *Macromolecules*, 50(10):3733–3749, 2017.

[7] Frank S Bates and Glenn H Fredrickson. Block copolymer thermodynamics: theory and experiment. *Annual review of physical chemistry*, 41(1):525–557, 1990.

[8] Leonel Barreda, Zhengyuan Shen, Qile P Chen, Timothy P Lodge, J Ilja Siepmann, and Marc A Hillmyer. Synthesis, simulation, and self-assembly of a model amphiphile to push the limits of block polymer nanopatterning. *Nano letters*, 19(7):4458–4462, 2019.

[9] Yangyang Sun and Fernando A Escobedo. Coarse-grained molecular simulation of bolapolyphiles with a multident lateral chain: Formation and structural analysis of cubic network phases. *Journal of Chemical Theory and Computation*, 20(4):1519–1537, 2023.

[10] Shaojie Bai, J Zico Kolter, and Vladlen Koltun. An empirical evaluation of generic convolutional and recurrent networks for sequence modeling. *arXiv preprint arXiv:1803.01271*, 2018.

[11] A Vaswani. Attention is all you need. *Advances in Neural Information Processing Systems*, 2017.

[12] Robin Rombach, Andreas Blattmann, Dominik Lorenz, Patrick Esser, and Björn Ommer. High-resolution image synthesis with latent diffusion models. In *Proceedings of the IEEE/CVF conference on computer vision and pattern recognition*, pages 10684–10695, 2022.

[13] Robert A Jacobs, Michael I Jordan, Steven J Nowlan, and Geoffrey E Hinton. Adaptive mixtures of local experts. *Neural computation*, 3(1):79–87, 1991.

[14] Michael I Jordan and Robert A Jacobs. Hierarchical mixtures of experts and the em algorithm. *Neural computation*, 6(2):181–214, 1994.

[15] Ryan S DeFever, Colin Targonski, Steven W Hall, Melissa C Smith, and Sapna Sarupria. A generalized deep learning approach for local structure identification in molecular simulations. *Chemical science*, 10(32):7503–7515, 2019.

[16] Zhengyuan Shen, Yangzesheng Sun, Timothy P Lodge, and J Ilja Siepmann. Development of a pointnet for detecting morphologies of self-assembled block oligomers in atomistic simulations. *The Journal of Physical Chemistry B*, 125(20):5275–5284, 2021.

[17] Zhengyuan Shen, Ke Luo, So Jung Park, Daoyuan Li, Mahesh K Mahanthappa, Frank S Bates, Kevin D Dorfman, Timothy P Lodge, and J Ilja Siepmann. Stabilizing a double gyroid network phase with 2 nm feature size by blending of lamellar and cylindrical forming block oligomers. *JACS Au*, 2(6):1405–1416, 2022.

[18] Litao Chen, Bingxu Wang, Wentao Zhang, Shisheng Zheng, Zhefeng Chen, Mingzheng Zhang, Cheng Dong, Feng Pan, and Shunning Li. Crystal structure assignment for unknown compounds from x-ray diffraction patterns with deep learning. *Journal of the American Chemical Society*, 146(12):8098–8109, 2024.

[19] Pengyu Chen and Kevin D Dorfman. Gaming self-consistent field theory: Generative block polymer phase discovery. *Proceedings of the National Academy of Sciences*, 120(45):e2308698120, 2023.

[20] Shuochen Zhao, Tianyun Cai, Liangshun Zhang, Weihua Li, and Jiaping Lin. Autonomous construction of phase diagrams of block copolymers by theory-assisted active machine learning. *ACS Macro Letters*, 10(5):598–602, 2021.

[21] Daniel Franke, Cy M Jeffries, and Dmitri I Svergun. Machine learning methods for x-ray scattering data analysis from biomacromolecular solutions. *Biophysical journal*, 114(11):2485–2492, 2018.

[22] Hao He, Can Liu, and Haiguang Liu. Model reconstruction from small-angle x-ray scattering data using deep learning methods. *Iscience*, 23(3), 2020.

[23] Magnus Röding, Piotr Tomaszewski, Shun Yu, Markus Borg, and Jerk Rönnols. Machine learning-accelerated small-angle x-ray scattering analysis of disordered two-and three-phase materials. *Frontiers in Materials*, 9:956839, 2022.

[24] Hongyan Hao, Yan Wang, Siqiao Xue, Yudi Xia, Jian Zhao, and Furao Shen. Temporal convolutional attention-based network for sequence modeling. *arXiv preprint arXiv:2002.12530*, 2020.

[25] Yang Lin, Irena Koprinska, and Mashud Rana. Temporal convolutional attention neural networks for time series forecasting. In *2021 International joint conference on neural networks (IJCNN)*, pages 1–8. IEEE, 2021.

[26] Noam Shazeer, Azalia Mirhoseini, Krzysztof Maziarz, Andy Davis, Quoc Le, Geoffrey Hinton, and Jeff Dean. Outrageously large neural networks: The sparsely-gated mixture-of-experts layer. *arXiv preprint arXiv:1701.06538*, 2017.

[27] William Fedus, Barret Zoph, and Noam Shazeer. Switch transformers: Scaling to trillion parameter models with simple and efficient sparsity. *Journal of Machine Learning Research*, 23(120):1–39, 2022.

[28] Thomas H Epps, Eric W Cochran, Travis S Bailey, Ryan S Waletzko, Cordell M Hardy, and Frank S Bates. Ordered network phases in linear poly (isoprene-b-styrene-b-ethylene oxide) triblock copolymers. *Macromolecules*, 37(22):8325–8341, 2004.

[29] Kaiming He, Xiangyu Zhang, Shaoqing Ren, and Jian Sun. Deep residual learning for image recognition. In *Proceedings of the IEEE conference on computer vision and pattern recognition*, pages 770–778, 2016.

[30] Mukund Sundararajan, Ankur Taly, and Qiqi Yan. Axiomatic attribution for deep networks. In *International conference on machine learning*, pages 3319–3328. PMLR, 2017.